Optical Image Acquisition, Analysis and Processing for Biomedical Applications

Daniel L. Farkas*, Byron Ballou, Congwu Du, Gregory W. Fisher, Christopher Lau, and Richard M. Levenson

Center for Light Microscope Imaging and Biotechnology,
Carnegie Mellon University, Pittsburgh PA 15213, USA

Light is a most versatile tool for investigating biological systems and phenomena; the range, non-destructiveness, spatial discrimination and speed of optical imaging are all important for investigating biological structure and function at the cellular, tissue or even whole organism level. In *live* biological imaging, where the technological requirements are heightened by the challenges posed, other features of light, such as coherence and wavelength, are used to generate the additional contrast and resolution needed. We report here the recent improvements in our ability to image biological specimens optically, focusing on (a) spectral imaging and the related image processing issues, and (b) tomographic three-dimensional fluorescence imaging *in vivo*.

1 Introduction

Light microscopy is one of the most established methods of investigation in research, to the extent that the microscope has become an icon of the sciences. Modern digital light microscopy workstations allow detailed, quantitative imaging of structures within cells [1] while automation and optimization of these instruments [2] make live monitoring of cellular dynamics possible. This basic biological information can be useful in more applied fields, such as biotechnology, pathology [3] and cancer research [4,5]. Almost all current imaging is intensity-based (whether transmitted light, fluorescence or luminescence are used). More recently, lifetime-based imaging has been introduced and applied to interesting cases. However, there are many other optical parameters and contrast mechanisms to consider, with associated imaging modalities; spectral imaging and optical tomography are such cases, and we address them here.

2 Optical Imaging in the Spectral Domain

2.1 Multiparameter/Multiwavelength Imaging. Current efforts concentrate on the use of immunological and molecular reagents for detection of specific intracellular gene-regulation events. "Read-out" can be achieved using either chromogenic or fluorescent labels. The advantages of the imaging approach are the ability to visualize directly the cells under study, the ability to localize cell constituents within individual cells (and co-localize them with other constituents within the same cells), the ability to enumerate discrete objects (chromosomes, gene loci) and, in tissue sections, the ability to make use of tissue microarchitectural information. Molecular characterization of tumors frequently requires that multiple analytes be detected, visualized and quanti-

fied in each cell, and it is highly desirable to be able to perform these measurements simultaneously. This requires the development of technology and protocols for multi-wavelength fluorescent molecular and immunological assays. However, resolution of more than 3 or 4 simultaneous colors in histological or cytogenetic preparations is difficult to achieve with typical fluorescence microscopy arrangements, due to the problem of spectral overlap among dyes, resulting in "leak-through" from one optical channel to another. The same difficulty is present for multi-color chromosome painting and molecular fluorescence *in situ* hybridization (FISH). However, advances in dye chemistry, filter technology, software and imaging instrumentation have opened up the possibility of resolving a large number of fluorescent probes simultaneously.

2.2 Spatially-Resolved Fourier Transform Spectroscopy

Spectral Filtering. Several approaches suitable for multi-color imaging analysis of clinical samples have been pursued. The main ones are: (a) switchable, multiple band-pass and/or narrow-pass optical filters ("filter-wheels"); (b) tuneable (acousto-optical or liquid crystal) filters [6]; and (c) interferometery. The filter-wheel approach has been designed to perform immunophenotyping and whole-genome karyotyping [7], but is not well suited for analysis of spectrally complex specimens typical of stained histological samples. In a recent review of current technologies [8], we concluded that acousto-optic tunable filters (AOTFs) hold the most promise for time-critical spectral imaging, and Fourier spectral imaging interferometry does the same for slower, fixed-specimen measurements. Spatially resolved Fourier spectral imaging has only recently been applied to the visible optical range, with of a new instrument (developed by Applied Spectral Imaging, Inc.) which can measure and store a complete spectrum at each pixel of an image. It allows a multiplicity of dyes with overlapping spectra to be imaged at the same time with relatively high spectral and spatial resolution, and has been used to perform multi-color spectral karyotyping [9] and to detect the presence of intrinsic and extrinsic fluorescent compounds in individual cells [10].

Principle of Operation. In a multispectral imaging microscope, each pixel is actually one of several hundred thousand microspectrometers which act simultaneously and independently. As a consequence, the instrument acquires interferogram data, subsequently transformed by a fast Fourier transform (FFT) into a spectral image "cube" (a spectrum at every pixel). It is the inherent mechanical stability of the Sagnac design [11] that permits interferometry-based spectroscopy, which had previously been limited to the infrared, to be used in the visible region. The spectral range of a measurement depends on the light source, the throughput of the optics and the spectral sensitivity of the detector CCD.

Signal-to-Noise. It can be difficult to acquire images over large spectral ranges due to a combination of limitations in the spectral imaging hardware and in the CCD. A typical CCD has maximum sensitivity to wavelengths towards the red-end of the visible range, dropping precipitously around 400 nm. With Fourier-transform-based imaging spectrometers, spectral ranges can be limited because they acquire a spectral image at all wavelengths simultaneously. Consequently, images at wavelengths with low light signals or low CCD sensitivity (or both) cannot be acquired for longer periods than images corresponding to light-rich spectral regions. However, with band-

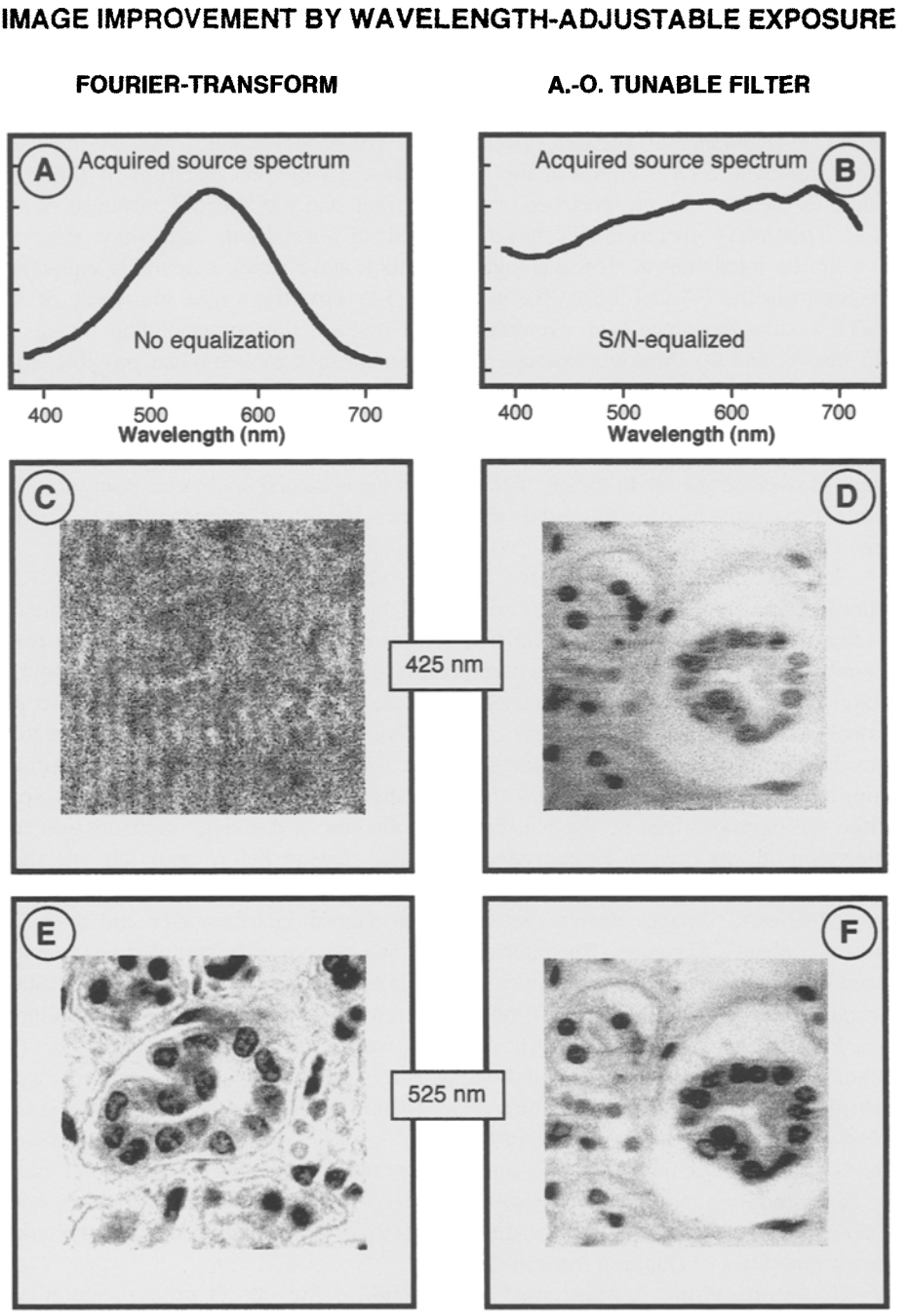

Fig. 1. Image improvement by wavelength-adjustable exposure. See text for explanation.

sequential devices, such as tuneable filter-based systems, exposure times for each spectral slice can be optimized, greatly improving signal-to-noise in the low- and high-wavelength regions. This is illustrated in Fig. 1, which compares spectral images of a hematoxylin and eosin-stained histological sections of kidney acquired by a FT-based system (left) and an AOTF-based system (right). The panels A and B indicate the spectrum recorded at a clear region of the image, thus giving the spectrum of the light source as modified by the presence of a blue filter and the spectral response of the CCD. The AOTF spectrum (B) shows the result of normalizing acquisition times to give similar intensities at all wavelengths. Panels E and F show essentially equivalent images from the FT and the AOTF system at 525 nm (the slight blurriness of the AOTF system has since been overcome [6]). However, the corresponding images at 425 nm (C and D) show the dramatic improvement in signal-to-noise possible with exposure optimization.

2.3 Computer Analysis of Spectrally Resolved Images. A multi-spectral image allows the viewer to locate, discriminate, measure and enumerate many entities within a specimen by detecting subtle differences among their individual spectral signatures [12].

Pixel-Unmixing. When the image is composed of combinations of well-defined spectral signals such as those emitted by fluorescently labeled compounds, spectral mixing can occur within the area imaged by a single pixel. This mixed-pixel phenomenon can also occur when a pure pixel is located at the object boundary (spatial mixture) and when the specimen contains more than one object along the microscopic optical path (depth mixture). Linear combination algorithms can assess the relative contribution of defined spectra to the signal recorded at each pixel, and by use of appropriate standards, can provide quantitation of absolute amounts for each label present. While this approach can be applied directly to fluorescence images, transmission and reflectance images need to be converted to optical density before applying the algorithm.

Methods. Images were acquired with a Sagnac interferometer and a frame-transfer cooled CCD camera. The interferometer and camera were mounted on an automated Zeiss Axioplan 2 microscope with infinity-corrected optics. The controlling computer was a Dell Pentium PC running Windows 3.1. The images were transferred to a Power Macintosh for analysis with software ("InSpectre") developed by the authors. Images are stored as 32-bit floating point numbers, so scaling artifacts from logarithm operations are not encountered during optical density conversions. For qualitative experiments in transmission, an Epson color ink-jet printer was used to generate microscopic overlapping ink dots (cyan and magenta) for imaging. A sample combining FISH and immunofluorescence was used to test the system in a mode not requiring conversion to optical density. Quantitative testing was performed by combining known quantities of fluors in the optical path.

Transmission. A transmitted light image of the ink-jet printer's output is shown in the top panel of Color Fig. 1. A spot where the cyan and magenta inks overlapped was imaged. The optical density conversion subtracted the background and inverted the image (note the elimination of the rough textured paper background signal).

Cyan and magenta spectra were chosen in the resulting image and then the linear combination algorithm was applied, yielding the two overlapping images on the right. On each separated image, the area where the dyes overlap has the same intensity as the areas where there is only a single dye. This is the expected result because a single unmixed dot is approximately uniform in intensity throughout its area. Spectral separations for transmission images should prove useful in the analysis of multi-colored immunohistochemistry samples.

Fluorescence. Presented here is a simple version of what we expect to be a major application of spectral imaging, namely, the quantitative segmentation of multiple, simultaneous FISH and immunofluorescent signals within single cells. The sample (a generous gift from Dr. S. Shackney) consisted of breast cancer cells stained for epidermal growth factor receptor (EGFR), using a fluorescently labeled antibody, and for chromosome 17 (a useful marker for aneusomy) by FISH. The spectral image was segmented using linear combination algorithms (Color Fig. 2), but since an example of the pure spectrum of the FISH probe was not available within this image (since it was everywhere mixed with the green antibody signal) the results of the segmentation left "holes" in the antibody image. Presumably, given a pure FISH spectrum, the algorithm should be able to separate the signals quantitatively and without overlap.

Quantitative Verification of Linear Combination Spectral Decomposition. To test whether spectral imaging is capable of quantitative deconvolving spectrally overlapping signals, we prepared known samples of dyes which

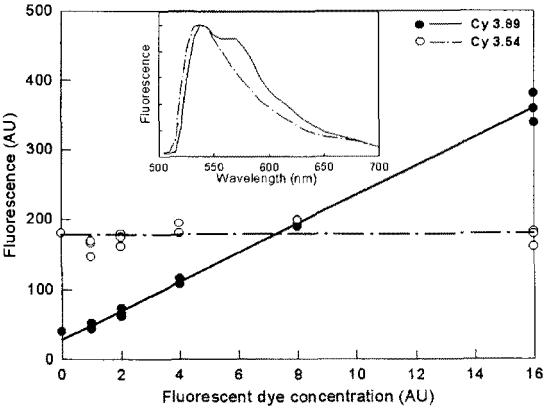

Fig. 2. Quantitative pixel-unmixing.

overlapped spatially and spectrally in a specially constructed cuvette with three chambers (only 2 of which were used for this application). Cy 3.54, a cyanine dye synthesized at our Center at Carnegie Mellon University and Rhodamine-6G were imaged together. From a 1:50 dilution of Rh-6G, dilutions of 1:250, 1:500, 1:1000, 1:2000, and 1:4000 were made. For each dilution, 3 measurements were taken. A 1:50 dilution of Cy 3.54 was present in the second chamber for each of the measurements. The pure spectra of Cy 3.54 and Rh-6G were used to apply the linear combination algorithm to each spectral mixture. Note the high degree of spectral overlap between the fluorescence emission signals of each dye. As can be seen, the presence of varying amounts

of Rh-6G did not affect the detection or quantitation of the constant levels of Cy 3.54. In the near-future, we expect to be able to quantitatively resolve the presence of 10 or more dye signals in multiply-labeled biological or pathological specimens.

3 *In Vivo* Imaging by Fluorescence Tomography

3.1 Light in Scattering Media. Research efforts are currently directed towards understanding how light, including fluorescence, can be generated and propagated within animal tissues. Migration and local intensities depend on (a) how the excitation and emitted light travel, (b) the *in situ* properties of the absorbing/emitting dye species, and (c) both the absorption and the scattering characteristics of the medium [13]. The factors which influence light propagation have only recently been modeled more accurately, in systems approaching biological tissues in complexity. Light scattering is usually modeled as a diffusive process, much like Brownian motion. Light can also

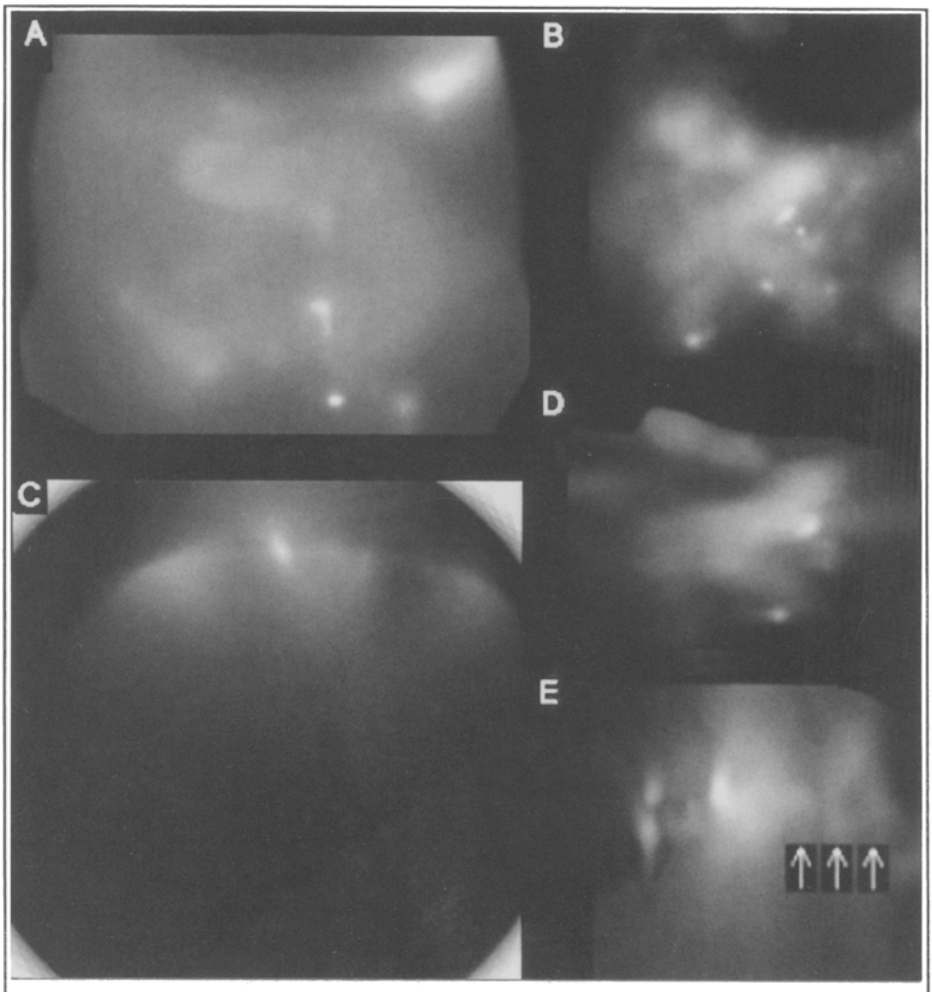

Fig. 3. Tomographic imaging in the mouse

be absorbed by a variety of biological macromolecules and thus fitting the Beer-Lambert relationship. Both absorption and scattering result in exponentially diminished light flux in any particular direction. In calculations, the amount of emitted light reaching the detector is given by the escape function. However, in an animal or human, this may not always describe light propagation adequately because bones and other tissues can affect transport along a path. To deal with this difficulty, we have performed optical tomography of fluorescence emission, viewing biological structures in back-projections to judge how deeply light penetrates in the nude mouse.

3.2 Back-Projection Fluorescence Tomography. This technique, not without difficulties, represents a reasonable compromise since information is obtained from many possible directions and merged into a single cross-section image. Only an outline of our method, similar to other emission tomographies, will be given here (for more details see [14]). We acquire fluorescence images with consecutive tilts ranging from -90° to +90° in 5° steps using a laser light source as excitation and a cooled CCD camera equipped with a special macro lens and emission filter for image recording. In these studies the camera was fixed above the specimen which was mounted on a platform and tilted. Tilts are aligned by making sinograms according to a principle proposed by Radon at the turn of the century.

To date, the best we have been able to resolve spatially in the nude mouse using fluorescence tomography is illustrated in Figure 3. Small, fluorescent beads emitting in the 700 nm range, were injected into the mouse peritoneum the previous day (Figure 3A) and were taken up into special lymphatics called Peyer's patches and into the small intestine overnight. The 0° tilt image is shown in Figure 3B. A back projection composed of 37 tilts is shown in Figure 3C, taken through a Peyer's patch. Rendering 125 rows of back projections is shown in Figure 3D. Note how similar the rendering shown in Figure 3D is to that in B of the same figure. An even more revealing aspect is shown in Figure 3E. Portions of several loops of intestines are clearly visible (arrows). Also, since images were spatially (depth) calibrated, we know that we are at least partially resolving down to 1 cm or more into the body, using 700 nm emission in the living nude mouse. We are currently investigating whether we can resolve even deeper if we use longer wavelength dyes (such as Cy7), whose emissions, in theory, should be less susceptible to image degradation due to light scattering.

4 Conclusion

We have demonstrated for a number of selected cases the usefulness of new approaches to optical imaging. The spatial discrimination, scattering rejection and spectral resolution of the imaging could all be increased in comparison with established techniques by a combination of optics, electronics and image processing, integrated in digital imaging workstations. We were able to demonstrate wavelength-resolved imaging for pathology, and *in vivo* fluorescence tomographic imaging in mice.

Acknowledgments. We would like to thank our colleagues at the Center for Light Microscope Imaging and Biotechnology for stimulating discussions and many

other forms of help. Support from the National Science Foundation (through grant NSF-MCB 8920118 to our Science and Technology Center), and from the Ben Franklin Technology Center of Western Pennsylvania is gratefully acknowledged.

References

1. Arndt-Jovin, D.J., Robert-Nicoud, M., Kaufman, S.J. and Jovin, T.M. (1985). Fluorescence digital microscopy in cell biology. Science, **230**: 247-256.

2. Farkas, D.L., Baxter, G., DeBiasio, R.L., Gough, A., Nederlof, M.A., Pane, D., Pane, J., Patek, D.R., Ryan, K.W. and Taylor, D.L. (1993). Multimode light microscopy and the dynamics of molecules. Ann. Rev. Physiol., **55**: 785-817.

3. Taylor, C.R. (1994). The current role of immunohistochemistry in diagnostic pathology. Adv. Path. Lab. Med., **7**: 59-105.

4. Folli, S., Westerman, P., Braichotte, D., Pelegrin, A., Wagnieres, G., Van Der Bergh, H. and Mach, J.P. (1994). Antibody-indocyanin conjugates for immunophotodetection of human squamous cell carcinoma in nude mice. Cancer Res., **54**: 2643-2649.

5. Ballou, B., Fisher, G.W., Waggoner, A.S., Farkas, D.L., Reiland, J.M., Jaffe, R., Mujumdar, R.B., Mujumdar, S.W. and Hakala, T.R. (1995). Tumor labeling *in vivo* using cyanine-conjugated monoclonal antibodies. Cancer Immunol. Immunother., **41**: 257-263.

6. Wachman, E.S., Niu, W. and Farkas, D.L. (1997). AOTF microscope for imaging with increased speed and spectral versatility. Biophysical Journal, **in press**.

7. Speicher, M.R., Gwyn Ballard, S. and Ward, D.C. (1996). Karyotyping human chromosomes by combinatorial multi-fluor FISH. Nat. Genet., **12**: 368-375.

8. Farkas, D.L., Ballou, B.T., Fisher, G.W. and Fishman, D. (1996). Microscopic and mesoscopic spectral bio-imaging. Proc. SPIE, **2678**: 200-209.

9. Schröck, E., du Manoir, S., Veldman, T., Schoell, B., Wienberg, J., Ferguson-Smith, M.A., Ning, Y., Ledbetter, D.H., Bar-Am, I., Soenksen, D., Garini, Y. and Ried, T. (1996). Multicolor spectral karyotyping of human chromosomes. Science, **273**: 494-497.

10. Malik, Z., Cabib, D., Buckwald, R.A., Talmi, A., Garini, Y. and Lipson, S.G. (1996). Fourier transform multipixel spectroscopy for quantitative cytology. J. Microsc., **182**: 133-140.

11. Garini, Y., Katzir, N., Cabib, D., Buckwald, R.A., Soenksen, D.G. and Malik, Z. (1996) *Spectral Bio-Imaging*. In: X.F. Wang and B. Herman (Editors), *Fluorescence Imaging Spectroscopy and Microscopy. Chemical Analysis Series, Vol. 137*. John Wiley & Sons, Inc.

12. Levenson, R.M. and Farkas, D.L. (1997). Digital spectral imaging for histopathology and cytopathology. SPIE, **2983**: 123-135.

13. Gardner, C.M., Jacques, S.L. and Welch, A.J. (1996). Light transport in tissue: Accurate expressions for one-dimensional fluence rate and escape function based upon Monte Carlo simulation. Lasers Surg Med, **18**: 129-138.

14. Farkas, D.L., Levenson, R.M., Ballou, B.C., Du, C., Lau, C., Wachman, E.S. and Fisher, G.W. (1997). Non-invasive image acquisition and advanced processing in optical bioimaging. Computerized Medical Imaging and Graphics, **in press**.

Quantitative Segmentation by Linear Combination

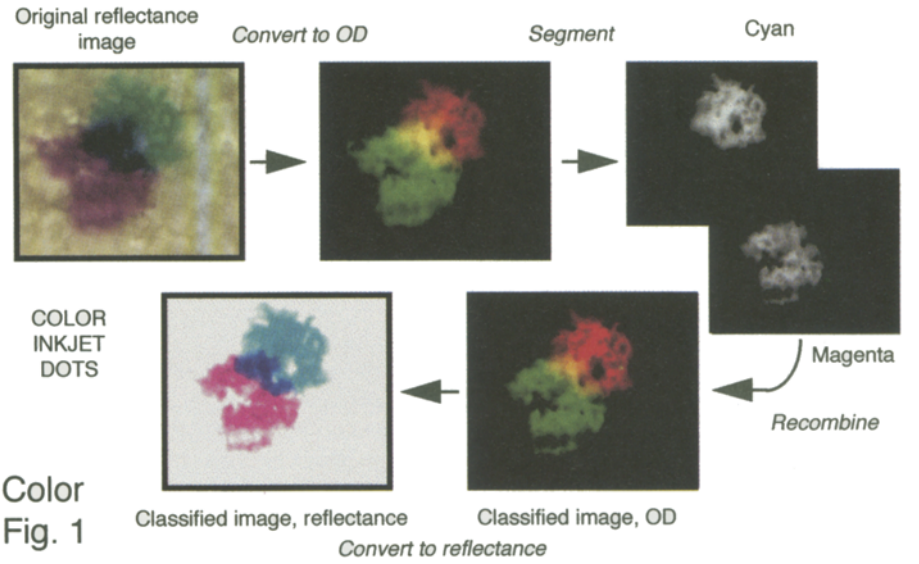

Color Fig. 1

Breast cancer: Combination immunofluorescence and FISH

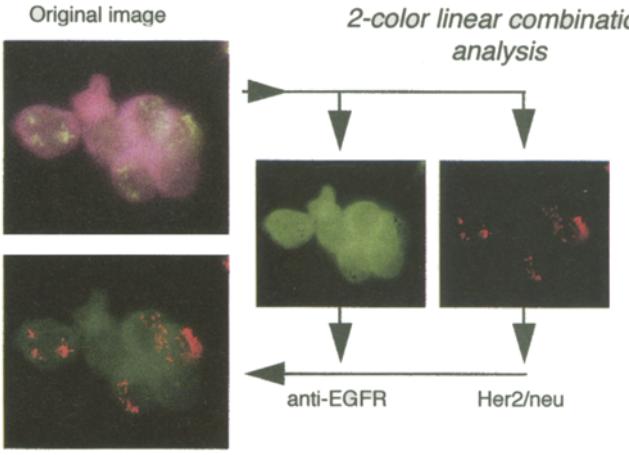

Color Fig. 2